

Old, Rich, and Eccentric: Two Jovian Planets Orbiting Evolved Metal-Rich Stars¹

KATHRYN M. G. PEEK,² JOHN ASHER JOHNSON,³ DEBRA A. FISCHER,⁴ GEOFFREY W. MARCY,² GREGORY W. HENRY,⁵
ANDREW W. HOWARD,² JASON T. WRIGHT,⁶ THOMAS B. LOWE,⁷ SABINE REFFERT,⁸ CHRISTIAN SCHWAB,⁸
PETER K. G. WILLIAMS,² HOWARD ISAACSON,⁴ MATTHEW J. GIGUERE⁴

kpeek@astron.berkeley.edu

Received 2009 March 20; accepted 2009 April 16; published 2009 May 16

ABSTRACT. We present radial velocity measurements of two stars observed as part of the Lick Subgiants Planet Search and the Keck N2K survey. Variations in the radial velocities of both stars reveal the presence of Jupiter-mass exoplanets in highly eccentric orbits. HD 16175 is a G0 subgiant from the Lick Subgiants Planet Search, orbited by a planet having a minimum mass of $4.4 M_{\text{Jup}}$, in an eccentric ($e = 0.59$), 2.71 yr orbit. HD 96167 is a G5 subgiant from the N2K (“Next 2000”) program at Keck Observatory, orbited by a planet having a minimum mass of $0.68 M_{\text{Jup}}$, in an eccentric ($e = 0.71$), 1.366 yr orbit. Both stars are relatively massive ($M_{\star} = 1.3 M_{\odot}$) and are very metal rich ($[\text{Fe}/\text{H}] > +0.3$). We describe our methods for measuring the stars’ radial velocity variations and photometric stability.

1. INTRODUCTION

Over 300 exoplanets have been detected to date,⁹ a quantity that is making it possible to characterize statistically significant trends that shed light on planet formation processes. Trends in planet occurrence as a function of host star mass and metallicity have emerged, and the distribution of orbital eccentricities is still being uncovered. For a review of exoplanet detections, see, e.g., Johnson (2009); Marcy et al. (2008); Udry et al. (2007).

Both the planet occurrence rate and the total planetary mass in a system are proving to be positively correlated with the host star’s mass (Johnson et al. 2007; Lovis & Mayor 2007). Our understanding of that planet occurrence rate at masses of $M_{\star} \geq 1.3 M_{\odot}$ comes from surveys of evolved stars. Intermediate-mass stars cool and slow their rotation as they evolve off the

main sequence, thereby developing the copious narrow metal lines that facilitate precision radial velocity monitoring. Since giant stars tend to have considerable photospheric jitter (introducing errors of $\sim 20 \text{ m s}^{-1}$), subgiants, which have jitters of $\sim 5 \text{ m s}^{-1}$, represent an evolutionary sweet spot for detecting planets around intermediate-mass stars.

In addition to correlating with stellar mass, the planet occurrence rate is observed to correlate with stellar metallicity (Fischer & Valenti 2005; Santos et al. 2004; Gonzalez 1997). The results of Doppler surveys are corroborated by theoretical predictions that more metals in a protoplanetary disk leads to more prolific planet formation (Ida & Lin 2004). This trend informs target selection for some exoplanet searches, e.g., the N2K program (“Next 2000,” Fischer et al. 2005) and the ELODIE Metallicity-Biased Planet Search (da Silva et al. 2006), which specifically target metal-rich stars. Such searches allow planet hunters to maximize exoplanet discoveries given finite telescope resources.

Exoplanet systems exhibit a broad range of eccentricities. For the 267 well-characterized planets within 200 pc (most of the known exoplanets), those in non-tidally-circularized orbits ($P > 5$ days) span a range of eccentricities from 0.00 to 0.93, with a median eccentricity of 0.23. The broad range of eccentricities is surprising, since it was previously expected that such objects would have orbits resembling the circular orbits of the solar system gas giants. The origin of exoplanet eccentricities is one of the major outstanding problems in the study of exoplanets. The discovery of additional planetary systems, especially those with large eccentricity, will bring the shape of the eccentricity distribution into better focus and guide theoretical models of planet formation and orbit evolution (e.g., Ford & Rasio 2008; Jurić & Tremaine 2008; Chatterjee et al. 2008).

¹Based on observations obtained at the Lick Observatory, which is operated by the University of California, and on observations obtained at the W. M. Keck Observatory, which is operated as a scientific partnership with the University of California, the California Institute of Technology, and the National Aeronautics and Space Administration. Keck Observatory was made possible by the generous financial support of the W. M. Keck Foundation. Keck time has been granted by both NASA and the University of California.

²Department of Astronomy, University of California, Berkeley, CA 94720-3411.

³Institute for Astronomy, University of Hawaii, Honolulu, HI 96822.

⁴Department of Physics and Astronomy, San Francisco State University, San Francisco, CA 94132.

⁵Center of Excellence in Information Systems, Tennessee State University, Nashville, TN 37209.

⁶Department of Astronomy, Cornell University, Ithaca, NY 14853.

⁷UCO/Lick Observatory, Santa Cruz, CA 95064.

⁸ZAH-Landessternwarte, Königstuhl 12, 69117 Heidelberg, Germany.

⁹See <http://www.exoplanets.org/>.

We present here two new Jupiter-mass exoplanets detected with the radial velocity method. Both stars are metal-rich ($[\text{Fe}/\text{H}] > +0.3$), intermediate-mass ($M_* = 1.3 M_\odot$), G-type subgiants, and therefore contribute to our understanding of the planet occurrence rate as a function of mass and metallicity. HD 16175 is part of the Lick Subgiants Planet Search (Johnson et al. 2006) and HD 96167 is part of the N2K program at Keck Observatory (Fischer et al. 2005). Because the planets presented here are from different programs at different observatories, we describe the observational, data analysis, and Keplerian techniques for each star in its own section. HD 16175 is presented in § 2 and HD 96167 in § 3. We review the photometric stability of the stars in § 4 and summarize our results in § 5.

2. HD 16175

2.1. Observations and Radial Velocity Measurements

We began Doppler monitoring of HD 16175 (HIP 12191, BD +41 496) at Lick Observatory in 2004 November as part of the Lick Subgiants Planet Search, a program comprising 159 evolved intermediate-mass stars, chosen to have color index $0.55 < B - V < 1.00$ mag, V -magnitude brighter than 7.6 mag, and declination $d > -20^\circ$. In order to choose evolved stars, we require an absolute visual magnitude M_V more than 1.0 mag above the main sequence. For this purpose, we use the main sequence defined in Wright 2005, which is a ninth-order polynomial fit to the *Hipparcos* dwarf stars within 60 pc. In order to ensure selection of subgiants rather than giants, we required M_V fainter than 1.0 mag. The color limits select stars for which radial velocity monitoring is feasible, while the V -magnitude and declination limits allow the sample to be observed with the 3 m Shane telescope and with the 0.6 m Coudé Auxiliary Telescope (CAT), both of which feed the Lick Observatory Hamilton echelle spectrograph (Vogt 1987). See Johnson et al. (2006) for a complete description of the Lick Subgiants Planet Search and its selection criteria.

We use the Hamilton spectrograph at a setting that provides resolution $R \approx 50000$ at $\lambda = 5500 \text{ \AA}$. On the CAT, typical exposure times were 60 minutes, yielding a signal-to-noise ratio (S/N) of ~ 50 at 5500 \AA . On the Shane, shorter 10 minute exposures generally yielded higher S/N ~ 175 . The lion's share of the data presented here were collected with the CAT. The procedure for obtaining radial velocities from Hamilton spectra is outlined in Butler et al. 1996. In short, a temperature-controlled Pyrex cell, filled with gaseous molecular iodine, is placed before the spectrometer's entrance slit. The iodine imprints a dense set of absorption lines between $\lambda \sim 5000 \text{ \AA}$ and $\lambda \sim 6400 \text{ \AA}$, which are calibrated to provide an accurate wavelength scale for each observation, and which also serve to provide information about the spectrometer's instrumental response (Marcy & Butler 1992).

The Doppler measurement method described here traditionally includes the use of a template spectrum, an iodine-free,

high-S/N observation relative to which the Doppler radial velocity measurements are made. In the case of HD 16175, we first measured the Doppler shifts relative to a synthetic "morphed" template spectrum. The procedure for creating the morphed template is described in Johnson et al. (2006). Once the star showed the potential for a planetary companion, we obtained a traditional template observation. The observed template is also used for the LTE analysis described in § 2.2.

The radial velocities, measured in approximately 700 2 Å segments of each echelle spectrum, are averaged to determine

TABLE 1
RADIAL VELOCITIES FOR HD 16175

JD -2,440,000	Radial velocity (m s ⁻¹)	Uncertainty (m s ⁻¹)
13338.681	81.17	5.96
13599.929	19.72	4.64
13629.867	5.4	4.73
13668.833	-10.57	4.96
13710.744	-48.24	5.36
13718.692	-46.62	5.26
13959.999	110.21	5.1
13966.942	81.34	6.02
13975.925	79.43	5.48
13998.914	104.92	5.44
14001.894	92.09	5.13
14020.897	92.71	5.89
14035.837	86.45	6.82
14046.831	90.77	5.27
14059.809	97.79	6.12
14099.808	90.56	5.14
14130.751	103.82	6.21
14136.648	93.97	5.58
14150.684	103.07	8.31
14170.642	72.56	5.83
14304.984	66.41	7.94
14309.978	71.15	4.79
14311.997	53.32	4.67
14336.958	61.7	4.57
14401.815	56.27	6.58
14404.904	55.17	11.24
14405.854	57.46	5.66
14417.794	30.49	7.8
14421.776	52.18	5.22
14422.837	56.29	5.96
14423.791	59.01	4.68
14425.847	64.05	5.06
14426.798	53.18	3.7
14525.640	20.61	7.68
14548.644	26.06	5.19
14675.985	-30.05	6.84
14677.971	-22.00	6.32
14699.954	-37.38	11.05
14734.937	-65.10	5.39
14748.784	-82.01	6.9
14767.935	-94.18	5.89
14846.680	38.5	5.49
14858.657	43.15	7.74
14904.639	78.14	7.19

the radial velocity of a star in a given observation. Table 1 contains the velocities and their associated uncertainties for HD 16175, from 2004 November to 2009 March. We estimate those uncertainties to be the standard deviation from the mean of the 700 individual segment velocities. Typical internal uncertainties for HD 16175 are $\sim 6 \text{ m s}^{-1}$. The internal uncertainties in Table 1 are added in quadrature to a 5 m s^{-1} error due to stellar jitter (a typical figure for subgiant stars; see Fischer et al. 2003 and Johnson et al. 2007), and those combined values are used in the least-squares Keplerian analysis described in § 2.3.

2.2. Stellar Properties

HD 16175 is a G0 subgiant in the foreground of galactic open cluster M34 (NGC 1039), which is 440 pc farther away. In our analysis we found several different V -band magnitudes HD 16175, so we adopted for our analysis here an average of the values from three sources: the Tereshchenko (2001) spectrophotometric standards list, the *Hipparcos* catalog (ESA 1997), and the Sky2000 catalog.¹⁰ Our adopted values were $V = 7.29 \pm 0.03$ and $B - V = 0.63 \pm 0.02$.

The *Hipparcos* parallax distance for HD 16175 is 60 ± 3 pc, which, when taken together with V from the preceding paragraph, implies an absolute visual magnitude $M_V = 3.40$. Its M_V places HD 16175 1.3 mag above the *Hipparcos* main sequence defined in Wright 2005 (a value that fulfills the selection criterion described in § 2.1). HD 16175's high metallicity (measured in the next paragraph) may account for part of its distance above the main sequence, but some of that 1.3 mag difference is likely due to its evolution, even though it may not yet have exhausted its core hydrogen.

HD 16175 is metal rich, with $[\text{Fe}/\text{H}] = +0.39 \pm 0.06$, and has an effective temperature $T_{\text{eff}} = 6080 \pm 70$ K. Metallicity and temperature come from our LTE spectral synthesis analysis with Spectroscopy Made Easy (SME; Valenti & Piskunov 1996). In general we follow the procedure outlined in Valenti & Fischer (2005). The LTE analysis also yielded surface gravity $\log g = 4.4 \pm 0.2$ and projected rotational velocity $v \sin i = 4.8 \pm 0.5 \text{ km s}^{-1}$. The uncertainties of the SME-derived stellar properties ($[\text{Fe}/\text{H}]$, T_{eff} , $\log g$, and $v \sin i$) were determined following the procedure described in Johnson et al. (2008) and Valenti & Fischer (2005). The full set of stellar properties and their uncertainties (in parentheses) appear in Table 2.

The stellar luminosity $L_* = 3.49 \pm 0.12 L_\odot$ was calculated using the relation in Valenti & Fischer (2005), based on M_V and a bolometric correction from (VandenBerg & Clem 2003). We follow the same procedure here, adopting a bolometric correction of -0.035 mag. The stellar radius $R_* = 1.68 \pm 0.04 R_\odot$ was calculated with the Stefan-Boltzmann law, using the L_* given and T_{eff} from the LTE analysis. We then calculated the stellar mass $M_* = 1.29 \pm 0.09 M_\odot$ and age 4.0 ± 1.0 Gyr

TABLE 2
STELLAR PARAMETERS

Parameter	HD 16175 ^a	HD 96167 ^a
V (mag)	7.29	8.09
M_V (mag)	3.4	3.46
$B - V$ (mag)	0.63	0.73
Distance (pc)	60 (3)	84 (9)
$[\text{Fe}/\text{H}]$	+0.39 (0.06)	+0.34 (0.06)
T_{eff} (K)	6080 (70)	5770 (70)
$v \sin i$ (m s^{-1})	4.8 (0.5)	3.8 (0.5)
$\log g$	4.4 (0.2)	4.0 (0.2)
M_* (M_\odot)	1.29 (0.09)	1.31 (0.09)
R_* (R_\odot)	1.68 (0.04)	1.86 (0.07)
L_* (L_\odot)	3.49 (0.12)	3.4 (0.2)
Bolometric Correction (mag)	-0.035	-0.081
Age (Gyr)	4.0 (1.0)	3.8 (1.0)
S_{HK}	0.17	0.14
$\log R'_{\text{HK}}$	-4.96	-5.16

^a Uncertainty given in parentheses.

using the Girardi et al. (2002) stellar interior models, based on the *Hipparcos*-derived M_V , the $B - V$ color, and the LTE-derived metallicity. The uncertainties for these derived values are propagated from the uncertainties on the input values.

The chromospheric activity parameters S_{HK} and $\log R'_{\text{HK}}$, based on the Ca II H and K emission features, are measured according to the procedure in Wright et al. (2004). The full listing of stellar characteristics for HD 16175 appears in Table 2.

2.3. Keplerian Fit

We search for the best fitting Keplerian orbital solution to the radial velocity time series with a Levenberg-Marquardt least-squares minimization. Beginning with a periodogram to determine an initial guess for the orbital parameters, our Keplerian fitter searches a grid of initial period guesses to determine the orbital solution. We estimate the uncertainties in those orbital parameters with a bootstrap Monte Carlo method: we subtract the best-fit Keplerian from the measured velocities, scramble the residuals and add them back to the original measurements, then obtain a new set of orbital parameters. We repeat this process for 1000 trials and adopt the standard deviations of the parameters from all trials as the formal uncertainties. For a more in-depth description of the Keplerian fitting and uncertainty determination procedures, see, e.g., Marcy et al. (2005).

For HD 16175, the best fitting Keplerian orbital solution has a period of $P = 990 \pm 20$ days (or 2.71 ± 0.05 yr). It also has eccentricity $e = 0.59 \pm 0.11$ and velocity semiamplitude $K = 94 \pm 11 \text{ m s}^{-1}$. The rms scatter of the data about the fit is 9.2 m s^{-1} , and the reduced $\sqrt{\chi^2_\nu}$ is 1.16. Based on our stellar mass estimate in § 2.2 of $M_* = 1.29 M_\odot$, the planet HD 16175 b has a semimajor axis $a = 2.1$ AU and a minimum planet mass $M_P \sin i = 4.4 M_{\text{Jup}}$. The full list of orbital parameters appears in Table 3, with their associated uncertainties in parentheses.

¹⁰ Vizie Online Data Catalog, 5109 (J. Myers et al., 2001).

TABLE 3
ORBITAL PARAMETERS

Parameter	HD 16175 b ^a	HD 96167 b ^a
P (d)	990 (20)	498.9 (1.0)
T_p ^b (JD)	2452820 (30)	2453057 (5)
e	0.59 (0.11)	0.71 (0.04)
K (m s ⁻¹)	94 (11)	20.8 (1.5)
ω (deg)	222 (9)	285 (7)
$M_p \sin i$ (M_{Jup})	4.4 (0.34)	0.68 (0.18)
a (AU)	2.1 (0.08)	1.3 (0.07)
Fit RMS (m s ⁻¹)	9.2	4.6
Jitter (m s ⁻¹)	5	5
Reduced $\sqrt{\chi^2}$	1.16	0.88
N_{obs}	44	47

^a Uncertainty given in parentheses.

^b Time of periastron passage.

The velocities from Table 1 are plotted in Figure 1. The error bars on the plot represent the quadrature addition of the internal measurement errors from Table 1 and 5 m s⁻¹ of stellar jitter (see § 2.1). The best-fit orbital solution is plotted with a dashed line and the orbital parameters are printed in the plot. The photometric stability and transit probability for HD 16175 b are discussed in § 4.

3. HD 96167

3.1. Observations and Radial Velocity Measurements

Doppler monitoring of HD 96167 (HIP 54195, BD -09 3201) began at Keck Observatory in January 2004 as part of the N2K consortium observing program. N2K targeted 2000 stars within 110 pc with the goal of detecting high transit probability hot Jupiters. The stars were chosen to have $0.4 < B - V < 1.2$ mag and V brighter than 10.5 mag. The targets were

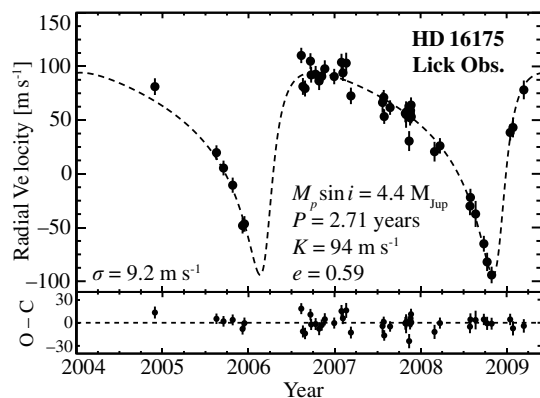


FIG. 1.—Radial velocity time series for HD 16175, measured at Lick Observatory. The error bars represent a quadrature sum of the internal measurement error (listed in Table 1) and 5 m s⁻¹ stellar jitter (see § 2.3 for more details). The dashed line represents the best Keplerian orbital fit to the data for HD 16175 b. The parameters of that fit are printed in the plot inset. The residuals between the Keplerian fit and the data appear in the lower panel of the plot.

also chosen to be metal rich, with [Fe/H] of +0.1 or higher, as determined photometrically (Ammons et al. 2006) and with low-resolution spectroscopy (Robinson et al. 2006). Observations of each star were collected in a high-cadence time series intended to detect short-period planets. For a full description of the N2K consortium and its goals, see Fischer et al. 2005. The main phase of the N2K program has finished, but several stars that showed significant velocity scatter have been monitored further. A number of longer period planets have been detected around these stars, including the planet orbiting HD 96167 announced here.

HD 96167 was observed with the HIRES echelle spectrograph (Vogt et al. 1994) on Keck I. The spectra have $R \approx 70000$ at $\lambda = 5500$ Å. The typical exposure time was 2 minutes, yielding S/N ~ 250 at 5000 Å. The iodine cell procedure for measuring radial velocities in Keck spectra is the same as for Lick spectra, described in § 2.1. As with the Lick Subgiants Planet Search, we initially observed the N2K stars relative to a morphed synthetic template spectrum (see § 2.1), taking a traditional template exposure once a planet candidate emerged.

The full list of measured velocities and their associated internal uncertainties (estimated as described in § 2.1) appears as Table 4. The observations span the period from 2004 January to 2009 January. Typical uncertainties are ~ 1 m s⁻¹, and a jitter uncertainty of 5 m s⁻¹ (Fischer et al. 2003; Johnson et al. 2007) is added in quadrature before the least-squares Keplerian fit is carried out (§ 3.3).

3.2. Stellar Properties

HD 96167 is a G5 subgiant star. In contrast to HD 16175, literature V -band magnitudes for HD 96167 were consistent with *Hipparcos*, so we adopt the *Hipparcos* values here: $V = 8.09$ and $B - V = 0.73$.

HD 96167 has a *Hipparcos* parallax-based distance of 84 ± 9 pc. The parallax distance and V -magnitude, when taken together, yield $M_V = 3.46$, placing it 1.5 mag above the main sequence as defined by the Wright (2005) polynomial. HD 96167's high metallicity (measured see next paragraph) may account for part of its distance above the main sequence, but its M_V places it far enough along the evolutionary track for 1.3- M_{\odot} stars that it has likely exhausted its core hydrogen and evolved into a subgiant.

Fitting with its inclusion in the N2K stellar sample, HD 96167 is metal rich, with [Fe/H] = $+0.34 \pm 0.06$, and has a near-solar temperature $T_{\text{eff}} = 5770 \pm 70$ K. It has $\log g = 4.0 \pm 0.2$ and $v \sin i = 3.8 \pm 0.5$ km s⁻¹. Its mass is $1.31 \pm 0.09 M_{\odot}$ and its age is 3.8 ± 1.0 Gyr; it has a luminosity L_{\star} of $3.4 \pm 0.2 L_{\odot}$ and radius R_{\star} of $1.86 \pm 0.07 R_{\odot}$. Its Ca II H and K chromospheric activity is relatively quiet, with $S_{\text{HK}} = 0.14$ and $\log R'_{\text{HK}} = -5.16$. As with HD 16175, the [Fe/H], T_{eff} , $\log g$, and $v \sin i$ come from an LTE spectral synthesis using SME. The procedures for determining L_{\star} , R_{\star} , M_{\star} , age, S_{HK} , and $\log R'_{\text{HK}}$ and their associated uncertainties are identical

TABLE 4
RADIAL VELOCITIES FOR HD 96167

JD -2,440,000	Radial Velocity (m s ⁻¹)	Uncertainty (m s ⁻¹)
13015.110	-18.65	1.99
13016.127	-22.75	1.82
13017.114	-21.43	1.98
13044.149	-12.93	1.48
13046.017	-17.81	1.62
13069.005	19.73	2.12
13073.938	21.05	2.32
13153.798	0.74	1.7
13195.752	-9.08	1.51
13196.783	4.47	1.53
13197.766	3.06	1.56
13369.127	-8.74	1.18
13370.114	7.48	1.33
13398.012	-13.93	1.14
13398.943	-13.28	1.11
13400.962	-15.04	1.1
13424.993	-11.88	1.03
13425.941	-16.44	1.16
13427.978	-15.67	1.2
13428.094	-13.57	1.14
13431.095	-13.24	1.1
13478.938	-15.86	1.2
13480.838	-14.61	1.11
13483.769	-18.05	1.16
13546.752	-9.70	1.62
13724.121	2.03	1.09
13748.102	-5.92	1.37
13753.044	-1.56	0.82
13754.051	-7.94	0.94
13775.991	-0.60	1.24
13776.990	-4.41	1.58
13806.985	-9.75	1.6
14131.028	8.9	1.5
14216.853	4.74	1.63
14248.838	1.79	1.41
14428.146	-10.12	1.05
14429.120	-13.51	1.15
14493008	-20.36	1.17
14547.913	-2.72	1.1
14548.850	-6.34	1.96
14602.805	18.48	1.4
14603.795	12.53	1.46
14639.781	6.98	1.34
14806.156	4.27	1.66
14811.120	-6.34	1.25
14839.123	-8.13	1.28
14847.065	-15.94	1.31

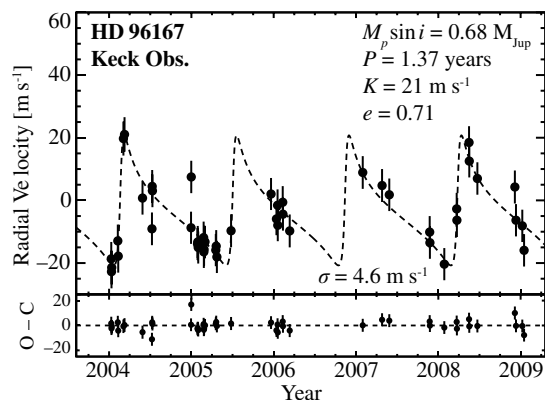


FIG. 2.—Radial velocity time series for HD 96167, measured at Keck Observatory. The error bars represent a quadrature sum of the internal measurement error (listed in Table 4) and 5 m s⁻¹ stellar jitter (see § 3.3 for more detail). The *dashed line* represents the best Keplerian orbital fit to the data for HD 96167 b. The parameters of that fit are printed in the plot inset. The residuals between the Keplerian fit and the data appear in the lower panel of the plot.

$P = 498.9 \pm 1.0$ days (or 1.366 ± 0.003 yr). The eccentricity e is 0.71 ± 0.04 and the velocity semiamplitude K is 20.8 ± 1.5 m s⁻¹. The residuals from the best fit have an rms scatter of 4.6 m s⁻¹; the fit has a reduced $\sqrt{\chi^2_\nu}$ of 0.88. Based on the LTE-determined mass estimate (§ 3.2) of $M_\star = 1.31 M_\odot$, the planet HD 96167 b has semimajor axis $a = 1.3$ and minimum mass $M_P \sin i = 0.68 M_{\text{Jup}}$.

The HD 96167 radial velocities listed in Table 4 are plotted in Figure 2. As with HD 16175, the error bars represent the quadrature sum of the internal measurement uncertainties from Table 4 and stellar jitter of 5 m s⁻¹. The best-fit orbital solution appears as the dashed line in Figure 2. The photometric stability and transit probability for HD 96167 b are discussed in § 4.

4. PHOTOMETRIC MEASUREMENTS OF HD 16175 AND HD 96167

We have obtained three years of high-precision differential photometry of both HD 16175 and HD 96167 with the T12 0.8 m automatic photometric telescope (APT) at Fairborn Observatory. The APT detects short-term, low-amplitude brightness variability in solar-type stars due to rotational modulation in the visibility of photospheric starspots (e.g., Henry et al. 1995), as well as longer-term variations associated with stellar magnetic cycles (Henry 1999). We obtain photometric observations to establish whether observed radial velocity variations in a star are due to reflex motion caused by a planetary companion or due to the effects of stellar activity (e.g., Queloz et al. 2001; Paulson et al. 2004). Photometric observations can also lead to the detection of planetary transits and the direct determination of planetary radii, as in Winn et al. (2008).

We acquired 181 observations of HD 16175 between 2006 December and 2009 February and 319 observations of HD 96167 between 2004 November and 2007 May. The T12

to those described in § 2.2. The full set of stellar parameters is listed in Table 2.

3.3. Keplerian Fit

The procedure for determining the best fitting Keplerian orbital solution for the velocities listed in Table 4 is the same as described in § 2.3. The best fitting orbital solution has

TABLE 5
SUMMARY OF THE ENSEMBLE PHOTOMETRIC OBSERVATIONS

Star (1)	APT (2)	Date Range (JD -2,440,000) (3)	N_{obs} (4)	Yearly Mean (mag) (5)	σ (mag) (6)	σ_{mean} (mag) (7)
HD 16175	T12	14080–14172	47	0.41236	0.00123	0.00018
		14370–14533	86	0.41232	0.00160	0.00017
		14730–14881	48	0.41079	0.00124	0.00018
HD 96167	T12	13330–13511	130	0.98318	0.00136	0.00012
		13690–13886	124	0.98380	0.00144	0.00013
		14058–14255	65	0.98287	0.00107	0.00013

APT uses two temperature-stabilized EMI 9124QB photomultiplier tubes to measure photon count rates simultaneously through Strömgren b and y filters. On a given night, the telescope observes each target star and three nearby comparison stars, along with measures of the dark count rate and sky brightness in the vicinity of each star. Designating the comparison stars as A, B, and C, and the target star as T, the observing sequence is as follows: dark, A, B, C, T, A, sky_A, B, sky_B, C, sky_C, T, sky_T, A, B, C, T. For HD 16175, the comparison stars A, B, and C were HD 16176, HD 14095, and HD 14064, respectively; for HD 96167, the comparison stars were HD 96220, HD 95938, and HD 94206. A diaphragm size of 45" and an integration time of 20 s were used for all integrations.

The measurements in each sequence were reduced to form three independent measures of the six differential magnitudes $T - A$, $T - B$, $T - C$, $C - A$, $C - B$, and $B - A$. These differential magnitudes were corrected for extinction and transformed to the standard Strömgren photometric system. To increase the S/N, the data from the b and y passbands were averaged to create " $(b + y)/2$ " magnitudes. After passing quality control tests, the three independent measures of each differential magnitude were combined to give a single mean data point per complete sequence for each of the six differential magnitudes.

To improve our measurement precision still further, we averaged the three mean $T - A$, $T - B$, and $T - C$ differential magnitudes from each sequence into a single value representing the difference in brightness between the program star and the mean of the three comparison stars $T - (A + B + C)/3$, which we refer to as the ensemble mean. This helps to average out any subtle brightness variations in the three comparison stars. The ensemble means for the three observing seasons of both stars are summarized in Table 5 and plotted as open circles in Figure 3.

Column 5 gives the yearly mean $T - (A + B + C)/3$ differential magnitudes in $(b + y)/2$ for the three observing seasons. Column 6 gives the standard deviations, σ , of these ensemble differential magnitudes from the yearly mean, providing a measure of night-to-night brightness variations. Typical standard deviations for constant stars fall in the range 0.0012–0.0017 mag for this telescope. All six of the standard deviations in Table 5

fall within this range. Periodogram analyses of the three observing seasons for each star found no significant periodicity in the range of 1–100 days. Both HD 16175 and HD 96167 are constant from night to night to the limit of our measurement precision; stellar activity due to starspots should have no significant effect on the measured radial velocities.

The standard deviations of the yearly means are given in Table 5, column 7, computed from the σ in column 6 divided by the square root of the number of observations in column 4; these values provide an estimate of the precision of each yearly mean. The observed yearly means are plotted in Figure 3 as filled circles connected with solid line segments. For both HD 16175 and HD 96167, the observed scatter in the yearly

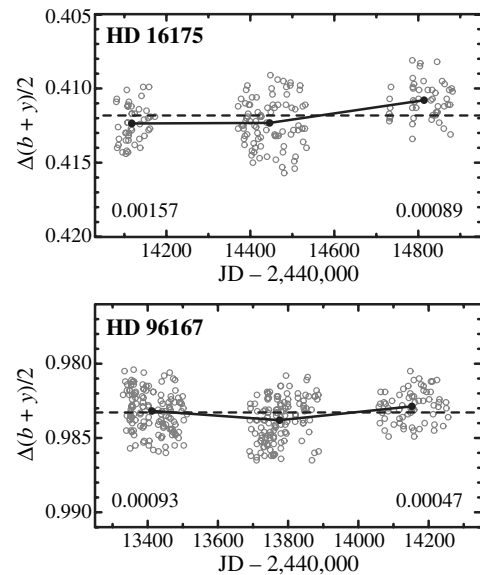


FIG. 3.—Nightly mean differential magnitudes of both stars (*open circles*). The yearly means are plotted as *filled circles* connected with *straight line* segments. The *dashed line* in each panel represents the mean of the three yearly means. The total range in magnitudes of the three yearly means is given in the lower left corner of each panel. The standard deviation of the yearly means from the mean of the means (*dashed lines*) is given in the lower right corner.

means is somewhat higher than the estimated precision of the means, by factors of 5.0 and 3.7, respectively, implying that there are slight year-to-year variations in the brightness of the two stars. Henry 1999 demonstrates that subtle brightness variability can be measured for solar-type stars and also demonstrates observationally that yearly means of constant stars can be measured to 0.0002 mag with the APTs. Wright et al. 2008 includes another example of this measurement precision for comparison stars. Thus, the long-term variation over a range of 0.0016 mag in HD 16175 is likely to be real. The range for HD 96167 is less than a millimagnitude over the three observing seasons and so is harder to establish as real without a longer time series. As subgiants with very low chromospheric activity levels (S_{HK} and $\log R'_{\text{HK}}$ in Table 2), both stars are expected to have little brightness variation. Given the moderately long orbital periods and the current precision of the orbits, a transit search is premature.

5. SUMMARY

We present here two Jovian-mass planets in relatively long period, eccentric orbits around intermediate-mass stars with supersolar metallicity. HD 16175 is a $1.29-M_{\odot}$ G0 subgiant from the Lick Subgiants Planet Search at Lick Observatory, orbited by a planet with a minimum mass of $4.4 M_{\text{Jup}}$ in a 2.71 yr, eccentric ($e = 0.59$) orbit. HD 96167 is a $1.31-M_{\odot}$ G5 subgiant from the N2K program at Keck Observatory, orbited by a planet with a minimum mass of $0.68 M_{\text{Jup}}$ in a 1.366 yr, eccentric ($e = 0.71$) orbit. The relatively high metallicities and masses of the stars in question make these planets particularly interesting additions to the exoplanet menagerie.

Approximately half of the planets orbiting subgiants detected to date are in orbits longer than a year. HD 16175 b and HD 96167 b are additions to that category, with periods of 2.71 ± 0.05 and 1.366 ± 0.003 yr, respectively. Of the 267 known Doppler exoplanets with well-constrained orbits within 200 pc,

23 are in orbits more eccentric than HD 16175 b ($e = 0.59$) and only 12 are in orbits more eccentric than HD 96167 b ($e = 0.71$). Only eight of the known Doppler planets orbit stars more metal-rich than HD 16175 ($[\text{Fe}/\text{H}] + 0.39$), while only 23 orbit stars more metal-rich than HD 96167 ($[\text{Fe}/\text{H}] + 0.34$). The planets fall into the upper reaches of three emerging trends in exoplanet distribution (eccentricity, host star mass, and metallicity), thereby contributing to our understanding of the nature of exoplanets and of planet formation.

We are indebted to the many observers who collected spectra of these stars. For HD 16175, we thank the observers Kelsey Clubb, Julia Kregenow, Joshua Peek, Karin Sandstrom, and Julien Spronck. For HD 96167, we thank the observers Gaspar Bakos, R. Paul Butler, Chris McCarthy, Guillermo Torres, Steven S. Vogt, and Joshua Winn. We gratefully acknowledge the dedication and support of the Lick and Keck Observatory staffs, in particular Tony Misch for support with the Hamilton Spectrograph and Grant Hill and Scott Dahm for support with HIRES. JAJ is an NSF Astronomy and Astrophysics Postdoctoral Fellow with support from the NSF grant AST-0702821. DAF acknowledges research support from NASA grant NNX08AF42G. GWH acknowledges that Automated Astronomy at Tennessee State University has been supported by NASA and NSF as well as Tennessee State University and the State of Tennessee through its Centers of Excellence program. We thank the NASA Exoplanet Science Institute (NExSci) for support through the KPDA program. We thank the NASA, NOAO, and UCO/Lick telescope assignment committees for allocations of telescope time. The authors extend thanks to those of Hawaiian ancestry on whose sacred mountain of Mauna Kea we are privileged to be guests. Without their kind hospitality, the Keck observations presented here would not have been possible. This research has made use of the SIMBAD database, operated at CDS, Strasbourg, France, and of NASA's Astrophysics Data System Bibliographic Services.

REFERENCES

- Ammons, S. M., Robinson, S. E., Strader, J., Laughlin, G., Fischer, D., & Wolf, A. 2006, *ApJ*, 638, 1004
- Butler, R. P., Marcy, G. W., Williams, E., McCarthy, C., Dosanji, P., & Vogt, S. S. 1996, *PASP*, 108, 500
- Chatterjee, S., Ford, E. B., Matsumura, S., & Rasio, F. A. 2008, *ApJ*, 686, 580
- da Silva, R., Udry, S., Bouchy, F., Mayor, M., Moutou, C., Pont, F., Queloz, D., et al. 2006, *A&A*, 446, 717
- ESA 1997, *The Hipparcos and Tycho Catalogues*, (ESA SP-1200; Garching: ESA)
- Fischer, D. A., Laughlin, G., Butler, P., Marcy, G., Johnson, J., Henry, G., Valenti, J., et al. 2005, *ApJ*, 620, 481
- Fischer, D. A., Marcy, G. W., Butler, R. P., Vogt, S. S., Henry, G. W., Pourbaix, D., Walp, B., et al. 2003, *ApJ*, 586, 1394
- Fischer, D. A., & Valenti, J. 2005, *ApJ*, 622, 1102
- Ford, E. B., & Rasio, F. A. 2008, *ApJ*, 686, 621
- Girardi, L., Bertelli, G., Bressan, A., Chiosi, C., Groenewegen, M. A. T., Marigo, P., Salasnich, B., & Weiss, A. 2002, *A&A*, 391, 195
- Gonzalez, G. 1997, *MNRAS*, 285, 403
- Henry, G. W. 1999, *PASP*, 111, 845
- Henry, G. W., Fekel, F. C., & Hall, D. S. 1995, *AJ*, 110, 2926
- Ida, S., & Lin, D. N. C. 2004, *ApJ*, 616, 567
- Johnson, J. A. 2009, *ArXiv e-prints*
- Johnson, J. A., Butler, R. P., Marcy, G. W., Fischer, D. A., Vogt, S. S., Wright, J. T., & Peek, K. M. G. 2007, *ApJ*, 670, 833
- Johnson, J. A., Marcy, G. W., Fischer, D. A., Henry, G. W., Wright, J. T., Isaacson, H., & McCarthy, C. 2006, *ApJ*, 652, 1724
- Johnson, J. A., Marcy, G. W., Fischer, D. A., Wright, J. T., Reffert, S., Kregenow, J. M., Williams, P. K. G., & Peek, K. M. G. 2008, *ApJ*, 675, 784

- Jurić, M., & Tremaine, S. 2008, *ApJ*, 686, 603
- Lovis, C., & Mayor, M. 2007, *A&A*, 472, 657
- Marcy, G. W., & Butler, R. P. 1992, *PASP*, 104, 270
- Marcy, G. W., Butler, R. P., Vogt, S. S., Fischer, D. A., Henry, G. W., Laughlin, G., Wright, J. T., & Johnson, J. A. 2005, *ApJ*, 619, 570
- Marcy, G. W., Butler, R. P., Vogt, S. S., Fischer, D. A., Wright, J. T., Johnson, J. A., Tinney, C. G., Jones, H. R. A., et al. 2008, *Phys. Scr.*, T130, 014001
- Paulson, D. B., Saar, S. H., Cochran, W. D., & Henry, G. W. 2004, *AJ*, 127, 1644
- Queloz, D., Henry, G. W., Sivan, J. P., Baliunas, S. L., Beuzit, J. L., Donahue, R. A., Mayor, M., Naef, D., et al. 2001, *A&A*, 379, 279
- Robinson, S. E., Strader, J., Ammons, S. M., Laughlin, G., & Fischer, D. 2006, *ApJ*, 637, 1102
- Santos, N. C., Israelian, G., & Mayor, M. 2004, *A&A*, 415, 1153
- Tereshchenko, V. M. 2001, *Astron. Rep.*, 45, 1002
- Udry, S., Fischer, D., & Queloz, D. 2007, in *Protostars and Planets V*, ed. B. Reipurth, Reipurth, D. Jewitt, & K. Keil (Tucson: University of Arizona Press), 685–699
- Valenti, J. A., & Fischer, D. A. 2005, *ApJS*, 159, 141
- Valenti, J. A., & Piskunov, N. 1996, *A&AS*, 118, 595
- VandenBerg, D. A., & Clem, J. L. 2003, *AJ*, 126, 778
- Vogt, S. S. 1987, *PASP*, 99, 1214
- Vogt, S. S., Allen, S. L., Bigelow, B. C., Bresee, L., Brown, B., Cantrall, T., Conrad, A., Couture, M., et al. 1994, in *Proc. SPIE 2198, Instrumentation in Astronomy VIII*, ed. D. L. Crawford, & E. R. Craine, 362
- Winn, J. N., Henry, G. W., Torres, G., & Holman, M. J. 2008, *ApJ*, 675, 1531
- Wright, J. T. 2005, *PASP*, 117, 657
- Wright, J. T., Marcy, G. W., Butler, R. P., & Vogt, S. S. 2004, *ApJS*, 152, 261
- Wright, J. T., Marcy, G. W., Butler, R. P., Vogt, S. S., Henry, G. W., Isaacson, H., & Howard, A. W. 2008, *ApJ*, 683, L63